Polymer Degradation and Stability 149 (2018) 69–77

Contents lists available at ScienceDirect

Polymer Degradation and Stability

journal homepage: www.elsevier.com/locate/polydegstab

Flame-retarding epoxy resin with an efficient P/N/S-containing flame retardant: Preparation, thermal stability, and flame retardance

Pan Wang[a,1], Long Xia[a,1], Rongkun Jian[a,*], Yuanfang Ai[a], Xuelin Zheng[a], Guilin Chen[b,**], Junsheng Wang[c]

[a] Fujian Key Laboratory of Polymer Materials, College of Chemistry and Materials Science, Fujian Normal University, Fuzhou 350007, PR China
[b] Fujian Provincial Key Laboratory of Quantum Manipulation and New Energy Materials, College of Physics and Energy, Fujian Normal University, Fuzhou 350007, PR China
[c] Tianjin Fire Research Institute of the Ministry of Public Security, Tianjin 300381, PR China

ARTICLE INFO

Keywords:
Epoxy resin
Flame retardance
Thermal stability
Mechanism

ABSTRACT

To further study the effect of the phosphorus, sulfur, and nitrogen-containing flame retardant on epoxy resin, a DOPO-based phenol derivative 4-[(benzothiazolyl 2-amino)(6-oxido-6H-dibenz[c,e][1,2]oxaphosphorin-6-yl) methyl] phenol namely D-P-A, was successfully synthesized from 9, 10-dihydro-9-oxa-10-phosphaphenanthrene-10-oxide (DOPO), *p*-hydroxybenzaldehyde (PHBA), and 2-aminobenzothiazole (ABZ), and used to flame retard epoxy resin (EP). As expected, D-P-A imparted flame retardance to epoxy resin. For example, with 7.5 wt% loading of D-P-A, epoxy thermoset passed a UL-94 V-0 rating, and got a LOI value of 29.6%. Besides, D-P-A played an effective role in inhibiting heat release of EP, that EP/7.5% D-P-A showed a peak of heat release rate (PHRR) of 713 kW/m^2 much lower than 1137 kW/m^2 of EP. However, it decomposed in advance owing to the lower thermal stability of D-P-A. Finally, through Scanning electron microscopy (SEM), Raman spectra and X-ray photoelectron spectroscopy (XPS) and pyrolysis-gas chromatograph/mass spectrometer (Py-GC/MS), it disclosed that D-P-A exerted its flame-retardant activity both in the vapor and condensed phase.

1. Introduction

Epoxy resin (EP) is one of most popular thermosetting polymers, and widely used in coatings, adhesives, composites etc. Due to its good resistance to chemical and corrosion, low dielectric property and excellent mechanical strength [1–3]. While, it needs to satisfy the requirement of flame-retardant standard in some fields, since EP is flammable and cannot be self-extinguished, resulting in a high risk for people's lives and properties. Therefore, it is urgent to adopt proper ways to reduce the flammability of epoxy resins.

To achieve this aim, in the past decades, halogen-containing additives have been largely developed, and showed high effectiveness in flame-retarding polymers, while some of them are now restricted to use in consideration of their harm to the environment [4–7]. To date, lots of researchers have reported their own development in flame retarding epoxy resins, and series of work are presented. For example, epoxy nanocomposites with metal hydroxides [8,9] and carbon-family materials [10] are gradually becoming a focus. Although they have apparent improvement in terms of the cone calorimeter (CC) results, mechanical and thermal properties, they cannot give the direct answer to the flammability of epoxy resin. As for organic flame retardants, phosphorus [11,12] or phosphorus uniting other elements such as nitrogen [13–17], silicon [18–20], and sulfur [21–24] based flame retardants are now most prevalent due to their high efficiencies on enhancing the extinguished ability of epoxy resins. To date, DOPO based derivatives are largely reported to modify epoxy resins [25–30]. For instance, Wang reported a novel reactive DOPO-based triazol compound, and it imparted flame retardance to epoxy resin with 4 wt% loading [31]. Recently, it is reported by our group that P/N/S-containing flame retardants including DOPO-ABZ, D-AZ and DHBAZ (see Scheme 1) were effective on flame-retarding epoxy resins [23,32,33]. Inspired by the chemical structures of them, D-P-A with the similar structure is designed and used in epoxy resin. It is found that D-P-A also works well in flame-retarding epoxy resins; moreover, it shows less negative effect on the thermal stability of epoxy resin compared to DOPO-ABZ, D-AZ and DHBAZ, that EP/D-P-A has higher initial decomposition temperature than EP/DOPO-ABZ, EP/D-AZ and EP/DHBAZ with the same loading of flame retardants. In order to further understand the effect of this

* Corresponding author.
** Corresponding author.
E-mail addresses: jrkht1987@fjnu.edu.cn (R. Jian), glchen@fjnu.edu.cn (G. Chen).
[1] P. Wang and L. Xia contributed equally to this work.

https://doi.org/10.1016/j.polymdegradstab.2018.01.026
Received 26 October 2017; Received in revised form 21 January 2018; Accepted 28 January 2018
Available online 31 January 2018
0141-3910/

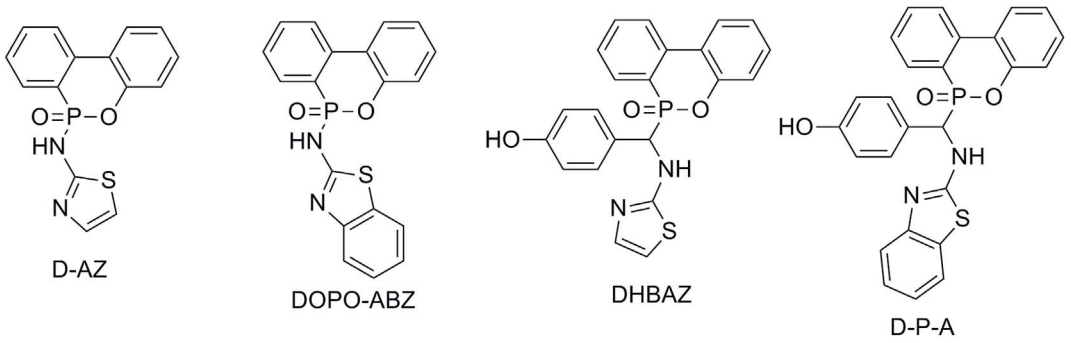

Scheme 1. The chemical structures of D-AZ, DOPO-ABZ, DHBAZ and D-P-A.

compound on epoxy resin, the detailed work has been carried out.

In this paper, a DOPO-based flame retardant namely D-P-A derived from DOPO, PHBA, and ABZ was synthesized through a two-step reaction. Then D-P-A was used to modify epoxy resin. The chemical structure of D-P-A was characterized and confirmed. Thermal properties of epoxy thermosets were studied. The flammability and combustion tests were experimented to assess the flame retardance and fire performance of flame-retardant epoxy thermosets. Finally, the flame retardant mechanism of D-P-A was also investigated.

2. Experimental

2.1. Materials

Diglycidyl ether of bisphenol-A (DGEBA, E-44) was available from Xingchen Synthetic Material Co., Ltd. (Nantong, China). 9, 10-Dihydro-9-oxa-10-phosphaphenanthrene-10-oxide (DOPO) was commercially obtained from Sunstar Technology Co., Ltd. (Huizhou, China). Absolute ethanol, 4, 4′-diamino-diphenylmethane (DDM) and *p*-hydroxybenzaldehyde (PHBA) were purchased from Sinopharm Chemical Reagent Co., Ltd. (Shanghai, China). 2-aminobenzothiazole (ABZ) was provided by Macklin Biochemical Co., Ltd. (Shanghai, China).

2.2. Synthesis of D-P-A

The synthetic route of D-P-A was shown in Scheme 2. To a 250 mL three-necked round-bottomed flask equipped with a magnetic stirrer, a reflux condenser, and a nitrogen inlet, 2-aminobenzothiazole (0.1 mol, 15.0 g) and *p*-hydroxybenzaldehyde (0.1 mol, 12.2 g) dissolved in 100 ml absolute ethanol were added and the solution were stirred at 50 °C for 2 h. Afterwards, the ethanol solution of DOPO (0.1 mol, 21.6 g) was gradually added into the reaction system accompanied with vigorous stirring. And then the reaction was kept at 50 °C for another 12 h. Finally, the solution was cooled down to the room temperature. The resulting precipitate was filtered, and then washed with ethanol under ultrasonic, and the process was repeated by twice. The product was dried at 80 °C for 8 h to obtain white powder (D-P-A, yield: 65%). FTIR (KBr, cm^{-1}), 3407 (-OH), 3227 (-NH-), 3034 (aromatic-H), 2918, 2811 (aliphatic C-H), 1601, 1529, and 1446 (benzene ring), 1220 (P = O). ^{1}H NMR (400 MHz, DMSO-d_6, ppm): 9.54, 9.51 (s, OH), 9.09, 8.99 (d, J = 9.6 Hz, N-H), 8.21–8.15 (m, 2H), 7.78–6.96 (m, 12H), 6.74–6.69 (m, 2H), 5.70, 5.41 (m, 1H); ^{31}P NMR (162 MHz, DMSO-d_6, ppm): 30.01, 28.58. HRMS (ESI^+): calcd. for $C_{22}H_{18}N_2O_3PS$ $[M+H]^+$ 471.0932, found 471.0896.

2.3. Preparation of EP/D-P-A samples

EP and D-P-A were firstly added to a stand-up flask, and mixed homogeneously at 130 °C for 30 min under rapid agitation using a mechanical stirrer. Secondly, after the solution was cooled down to 90 °C, DDM was added, and the mixture was vigorously stirred for 5 min. Then the resulting mixture was rapidly poured into preheated stainless steel molds and cured at 100 °C for 3 h, 150 °C for 2 h, and 180 °C for 2 h, respectively. Besides, EP obtained as a control was cured at 100 °C for 3 h and 150 °C for 2 h. It should be noted that the total amount of active protons of D-P-A and DDM used simultaneously as curing agents was equal to that of DDM used individually. The corresponding formulations of epoxy thermosets are listed in Table 1.

2.4. Characterization

The FTIR spectra of DOPO, PHB, ABZ and D-P-A were recorded in the range of 400–4000 cm^{-1} (KBr pellets) on a Thermo Nicolet 5700 FT-IR instrument. ^{1}H and ^{13}P NMR spectra of D-P-A were recorded on a Bruker AVANCE AV II-400 NMR instrument, and DMSO-d_6 was used as the solvent.

LOI tests were carried out through a HC-2C oxygen index meter (Jiangning, China) according to ASTM D2863, and the samples made into the dimensions of 130 mm × 6.5 mm × 3.2 mm were adopted; UL-94 vertical burning experiments were conducted through a CZF-2 instrument (Jiangning, China) according to ASTM D3801, and the samples with the dimensions of 130 mm × 13 mm × 3.2 mm were used. Burning behaviors were evaluated on a cone calorimeter device (Fire Testing Technology, East Grinstead, UK) according to ISO 5660-1, and the samples with dimensions of 100 mm × 100 mm × 3 mm were exposed to a radiant cone at a heat flux of 35 kW/m^2.

The glass transition temperature (T_g) was determined under nitrogen atmosphere by using a TA Q10 DSC instrument. The thermal

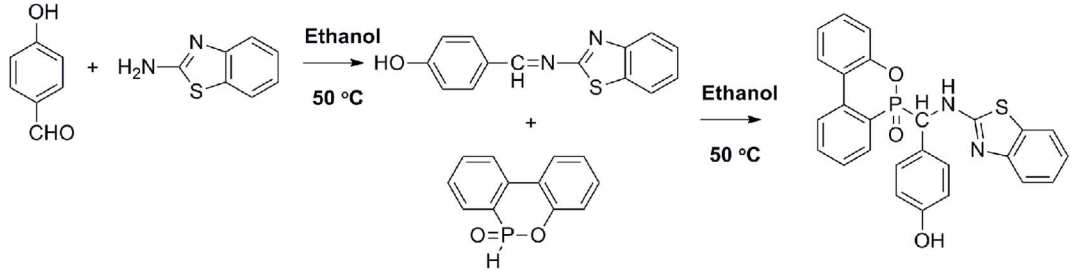

Scheme 2. Synthetic route of D-P-A.

Table 1
Formulations of epoxy thermosets and the results of UL-94 and LOI tests.

Samples	DGEBA (g)	DDM (g)	D-P-A (g)	P-content[a] (wt %)	UL-94 (3.2 mm)	LOI (%)
EP	100	25	0	0	No rating	25.1 ± 0.5
EP/5.0% D-P-A	100	20.44	6.32	0.33	V-1	29.3 ± 0.5
EP/7.5% D-P-A	100	19.74	9.73	0.50	V-0	29.6 ± 0.5
EP/10.0% D-P-A	100	18.96	13.33	0.66	V-0	31.5 ± 0.5

[a] $P(wt\%) = \frac{m_3}{m_1+m_2+m_3} \times \frac{31}{M} \times 100\%$; m_1, m_2, m_3 are equal to the mass of DGEBA, DDM and D-P-A respectively; M is the molecular weight of D-P-A.

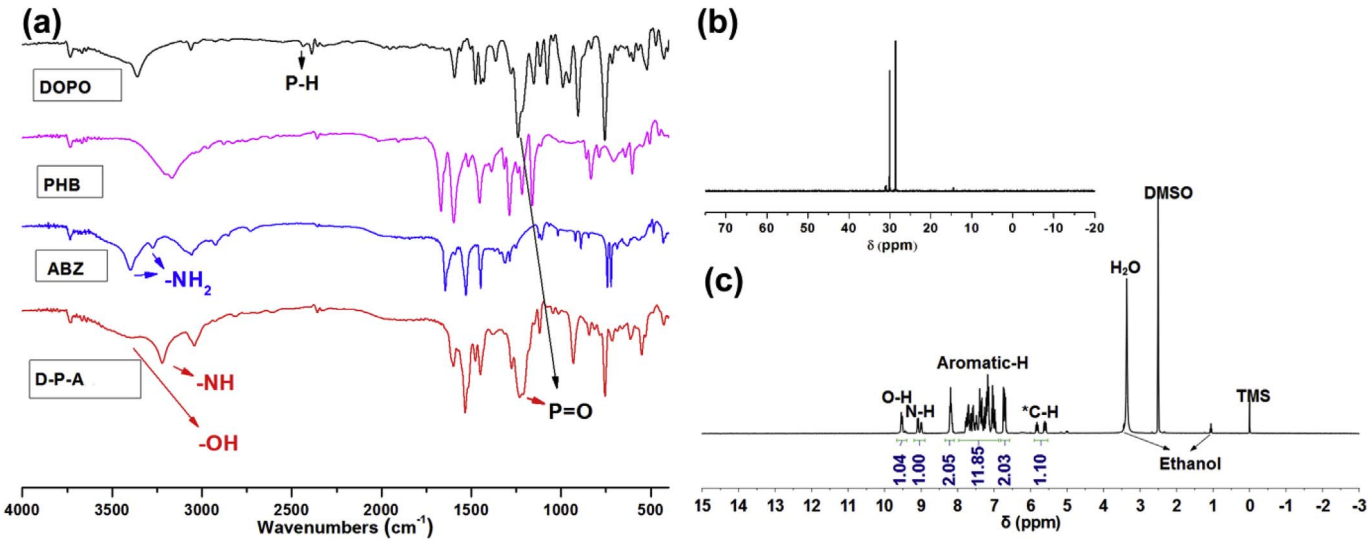

Fig. 1. FTIR (a), ^{31}P NMR (b) and ^{1}H NMR (c) spectra of D-P-A.

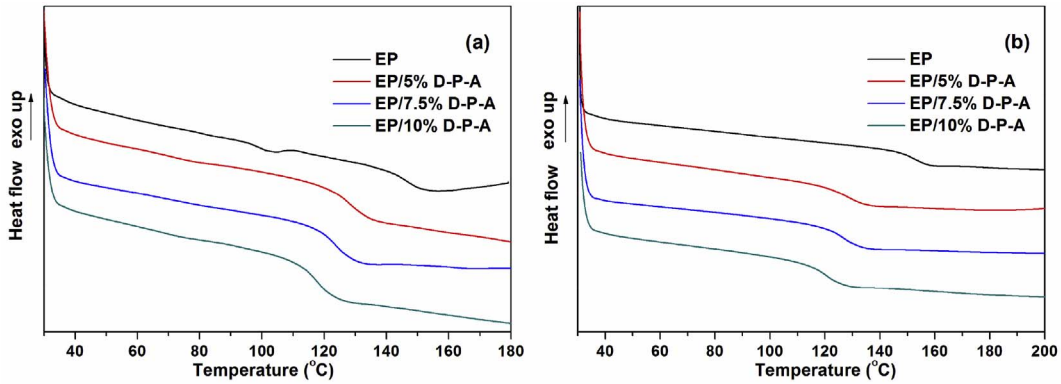

Fig. 2. First DSC heating scan (a); second DSC heating scan (b) of EP and EP/D-P-As.

Table 2
Thermal decomposition parameters of D-P-A, EP and EP/D-P-A formulations.

Samples	T_g (°C)	$T_{5\%}$ (°C)	T_{max} (°C)	Weight loss rate at T_{max} (wt %/min)	Residue at 800 °C (wt%)
D-P-A	–	227	275[1] 492[2]	6.1[a] 6.2[b]	28.5
EP	153	371	391	18.0	18.4
EP/5.0% D-P-A	128	343	378	12.1	19.5
EP/7.5% D-P-A	127	335	380	11.3	19.0
EP/10.0% D-P-A	121	337	376	10.4	21.6

[a] The first weight loss step of D-P-A from DTG.
[b] The second one of D-P-A from DTG.

history of epoxy thermosets were eliminated by heating to 180 °C and maintained at 180 °C for 3 min and then cooling down to 30 °C at a cooling rate of 10 °C/min. The T_g of epoxy thermosets were then determined by heating to 200 °C at a heating rate of 10 °C/min.

Thermal behaviors were assessed through a METTLER TGA/SDTA 851thermal analyzer in the temperature range of 30 °C–800 °C at a heating rate of 10 °C/min under nitrogen.

SEM observation on a HITACH S4800 was used to investigate the morphologies of char surfaces after CC tests of materials.

DXR laser Raman spectrometer using a 532 nm Helium-Neon laser line at room temperature was adopted to characterize the char residues.

The X-ray photoelectron spectroscopy (XSAM80, Kratos Co., UK) using Al Kα excitation radiation (hγ = 1486.6 eV) in ultrahigh vacuum conditions was carried out to analyze the component of char residues.

Py-GC/MS test was conducted on a Perkin-Elmer Clarus 680 GC-SQ8MS gas chromatography-mass spectrometer equipped with a CDS 5200 pyrolyzer. The helium (He) was utilized as carrier gas for the

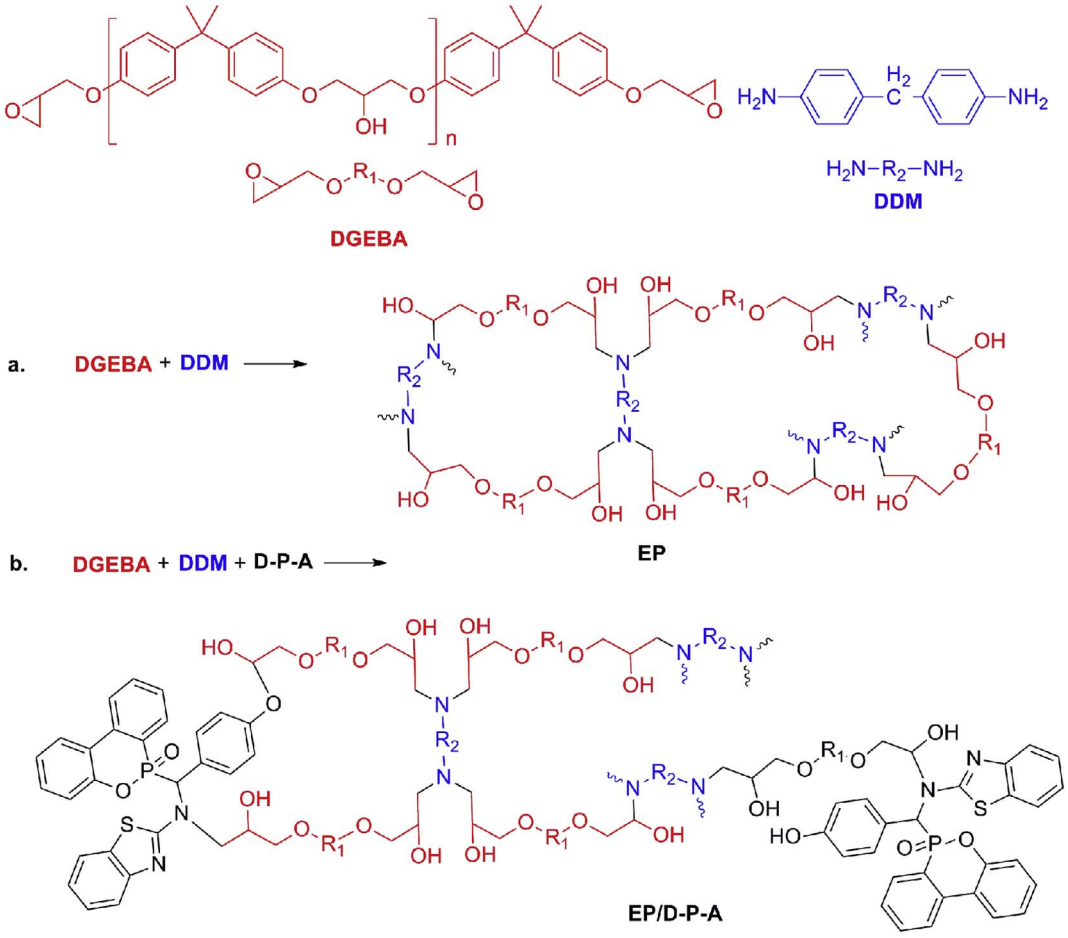

Fig. 3. The proposed chemical structures of EP and EP/D-P-A.

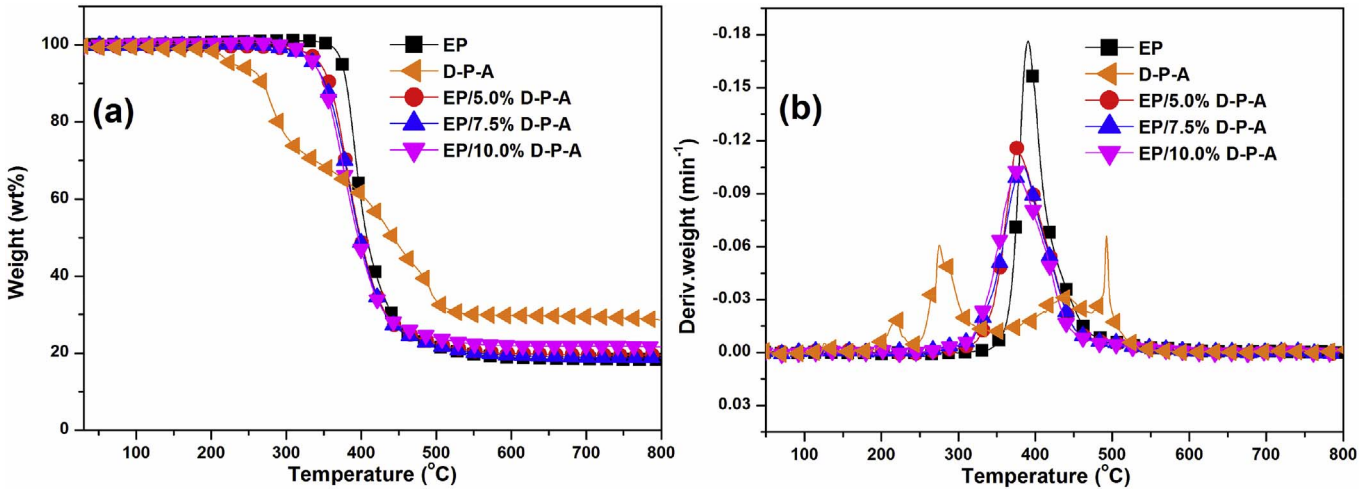

Fig. 4. TG (a) and DTG (b) curves of D-P-A, EP and EP/D-P-A formulations.

volatile products. The injector temperature was first kept at 40 °C for 3 min, and then the temperature was increased to 280 °C at a rate of 10 C/min. The temperature of GC/MS interface was 280 °C and the cracker temperature was 600 °C. MS indicator was operated in the electron impact mode at the electron energy of 70 eV, and the ion source temperature was kept at 250 °C. The identification of pyrolysis products were carried out according to NIST MS library.

3. Results and discussion

3.1. Synthesis of D-P-A

The chemical structure of D-P-A is characterized by FTIR, ^{1}H, and ^{31}P NMR in Fig. 1. Through comparing the FTIR spectra of DOPO, PHBA, ABZ, and D-P-A, it is clear that the absorption peaks around 2920 and 2961 cm^{-1} are assigned to the stretching vibration of methyne. The peaks at 3411, 3218, and 3036 cm^{-1} are due to the

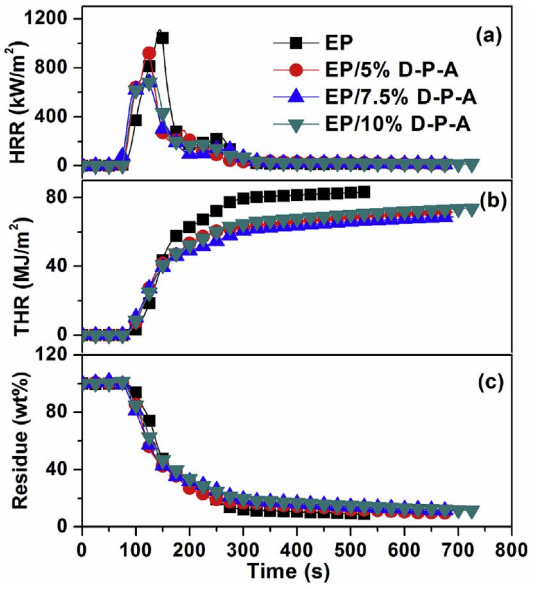

Fig. 5. HRR (a), THR (b) and Mass (c) against time curves of EP and EP/D-P-As.

Table 3
Burning parameters of EP and EP/D-P-As obtained from CC tests.

Sample	TTI (s)	PHRR (kW/m²)	THE (MJ/m²)	EHC (MJ/kg)	av-COY (kg/kg)	av-CO_2Y (kg/kg)	Residue (wt%)
EP	61	1137	83	22.3	0.095	1.634	8.7
EP/5% D-P-A	57	956	72	20.8	0.124	1.497	9.4
EP/7.5% D-P-A	67	713	69	20.5	0.104	1.207	11.4
EP/10% D-P-A	71	749	74	20.5	0.130	1.463	11.6

stretching vibration of -OH, -NH- and Ar-H, respectively. Moreover, P-C and P=O bonds also exhibit their absorbing signals at 1382 and 1224 cm^{-1}, indicating the existence of functional group in D-P-A. Besides, ^{1}H NMR depicted in Fig. 1(c) shows that there are two adjacent peaks for O-H, N-H and aliphatic C-H owing to the chiral carbon of D-P-A. In detail, the peaks at 9.54 and 9.51 ppm are attributed to O-H, the peaks at 9.10 and 8.98 ppm belong to the resonance of N-H, and the signals at 5.85 and 5.57 ppm are assigned to the hydrogen connecting with the chiral carbon. Besides, the multi-signals at 8.21–8.14, 7.78–6.96 and 6.74–6.69 ppm are due to the resonance of aromatic hydrogen. It is also worthy to note that the ratio of protons with different chemical environments matches well with the theoretical. Additionally, from the ^{31}P NMR spectrum of D-P-A, there are two signals located at 28.59 and 29.96 ppm. It should be noted that D-P-A is a chiral compound as it has a chiral carbon. Consequently, the phosphorus of D-P-A has two different chemical environments, leading to two chemical shifts. According to the analyses above, it confirms the successful synthesis of the target product D-P-A.

3.2. Thermal analysis

DSC tests are experimented to study the effect of D-P-A on the glass transition temperature of epoxy thermosets. From the first heating curves of EP and EP/D-P-As shown in Fig. 2(a), it is found that there is no exothermic peak in the whole process, indicating that the cross-linking reaction is complete, and epoxy resin is totally cured. The glass transition temperature (T_g) is determined by the second heating curves, and the T_g values of EP and EP/D-P-As are listed in Table 2. By comparison with EP, T_gs of EP/D-P-As are all decreased, due to that D-P-A also attends the curing process of epoxy resin via the reaction between –NH-, -OH and epoxy group, and the chemical structures of epoxy thermosets are sketched in Fig. 3, leading to the reduction of cross-linking density of epoxy thermosets. Besides, with the increasing addition of D-P-A, T_gs of epoxy thermosets are gradually decreased.

To explore the effect of D-P-A on decomposition behavior of epoxy resin, TG analyses are experimented under nitrogen atmosphere, and the results are shown in Fig. 4 and Table 2. As seen, the degradation range of D-P-A falls out between 200 and 500 °C, where two main weight-loss processes with maximum weight-loss rates (T_{max}) of 6.1 and 6.2 wt%/min at 275 °C and 492 °C. After the test, the amount of reserved residue at 800 °C is as high as 28.5%. As for EP, it experiences only one weight-loss stage with initial decomposition temperature ($T_{5\%}$) at 371 °C and the maximum weight-loss rate of 18.0 wt%/min at 387 °C. It is observed that in the presence of D-P-A, $T_{5\%}$ and T_{max} of epoxy thermosets are all decreased to some extent, owing to the lower thermal stability of D-P-A than that of EP. While, EPs modified with D-P-A exhibit similar thermal stability with the increasing amount of D-P-A, and they all show higher initial decomposition temperature than EP/DOPO-ABZ, EP/D-AZ and EP/DHBAZ systems [23,32,33], which might be due to the introduction of more rigid structure. It is noted that EP/D-P-A samples show a decrease in the weight-loss rates, and some increase in the residues at 800 °C compared to EP. Besides, the decomposition peaks of EP/D-P-As are all broadened, indicating that D-P-A can reduce the decomposition rate of EP, and extend the decomposition process of EP.

3.3. Fire performance

Flame retardance of EP and EP/D-P-As are assessed by LOI and UL-94 tests. As shown in Table 1, EP is a flammable polymer with LOI value of 25.1%, and it fails to pass a vertical UL-94 rating. When EP is modified with D-P-A, positive results are obtained. With 5 wt% amount of D-P-A in EP, the LOI value of the material increases to 29.3%, and it passes a vertical UL-94 V-1 rating. Moreover, it achieves a vertical UL-94 V-0 rating with the phosphorus content of only 0.5% for EP/7.5% D-

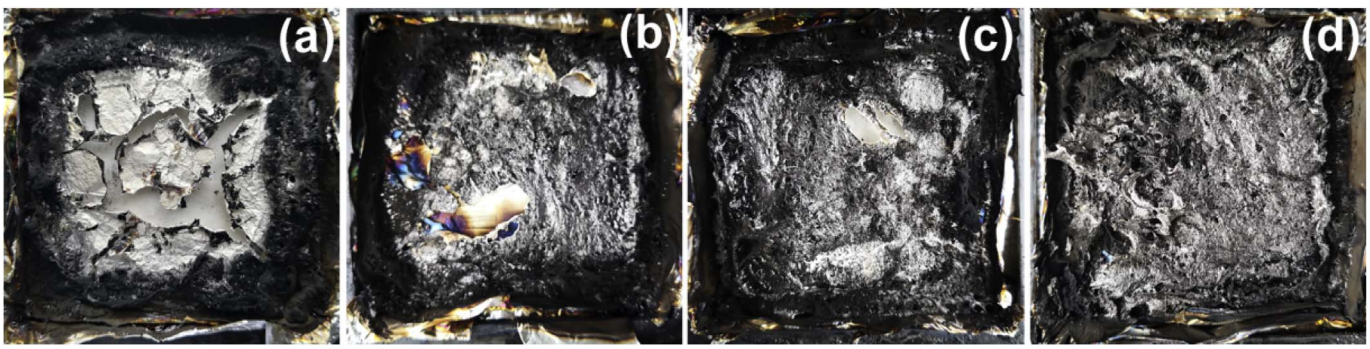

Fig. 6. The digital photos of the char residues of EP (a), EP/5% D-P-A (b), EP/7.5% D-P-A (c) and EP/10% D-P-A (d).

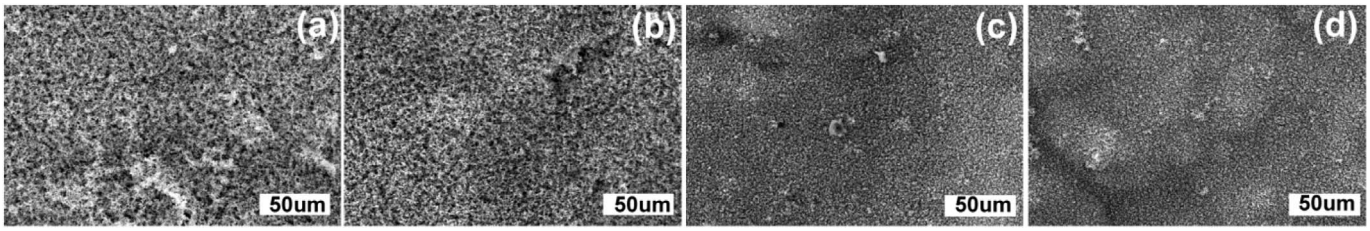

Fig. 7. Micro-morphologies of char residues for EP (a), EP/5% D-P-A, EP/7.5% D-P-A, and EP/10% D-P-A (d) after CC tests.

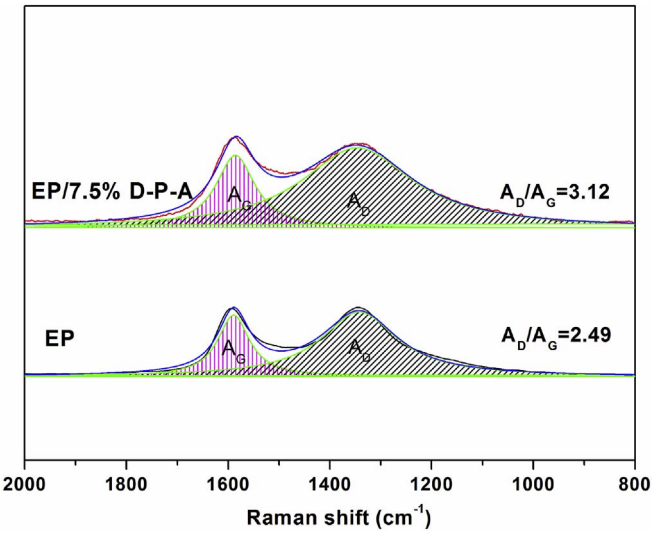

Fig. 8. The Raman spectra of EP and EP/7.5% D-P-A.

P-A. With further increasing the dosage of D-P-A, the LOI value of EP/D-P-A increases to 31.5%. The above suggests that D-P-A works well in flame-retarding epoxy resin.

Besides, to evaluate the effect of D-P-A on the burning behaviors of EP thermosets, CC tests are conducted on EP and EP/D-P-As, and the detailed results are shown in Fig. 5 and Table 3. EP releases much heat with a peak of heat release rate (PHRR) of 1137 kW/m^2. After combustion, EP exhibits a total heat evolved (THE) of 83 MJ/m^2. While, difference is observed after D-P-A is incorporated into EP. First of all, the PHRR values of EP/D-P-As are all lower than that of EP, and are decreased to 956, 713 and 749 kW/m^2. As compared with EP, the THE and av-EHC values of EP/D-P-As are also reduced, which is considered to be caused by the fuel-dilution and flame-inhibition function of D-P-A reducing the product of the effective heat of combustion of the volatiles and the combustion efficiency [34]. It can be further proofed by the values of av-COY and av-CO_2Y, that EP/D-P-As have a lower av-CO_2Y and a higher av-COY than EP. In other words, EP/D-P-As experience an incomplete combustion. Moreover, there is a great difference in the morphologies of EP and EP/D-P-As, which are shown in Fig. 6. In detail, the char residue of EP is not continuous and broken. With the addition of D-P-A, it can be found that the char morphologies are markedly improved, and the char are more continuous and compact, especially in the high loading of D-P-A. While in the higher loading of D-P-A, the effect of flame inhibition is not expected to be better. According to the above, it is reasonable to speculate the effectiveness of D-P-A on flame-retarding epoxy resin is related to the binary-activity in the vapor and condensed phase.

3.4. Flame-retardant mechanism

According to the results of CC tests, it is deduced that D-P-A exerts flame-retardant activity both in the vapor and condensed phase, thus SEM, Raman, XPS and Py-GC/MS are adopted to study the flame retardant mechanism of D-P-A.

3.4.1. Char residues analyses

According to the analyses of char macro-morphologies in the cone tests, it suggests that the char quality of EP/D-P-As show more improvement than that of neat EP. Therefore, SEM is adopted to observe the micro-morphologies of char residues after CC tests, and the results are shown in Fig. 7. As shown, the char layer of EP shows a shaggy and incompact morphology, indicating a poor effect on insulating the fuels, heat and oxygen. As for EP/D-P-As, although the micro-morphology of EP/5% D-P-A is not compact enough, while the char layers prone to exhibit more compact morphologies with the increasing loading of D-P-A, which could act better than that of EP as an insulating barrier to retard the oxygen and feedback of heat flux during combustion. Consequently, it coincides with the results of cone tests, and D-P-A can effectively flame-retard epoxy resin through the condensed activity.

Raman spectroscopy is a very effective tool to analyze the degree of structural disorder of carbonaceous materials [35,36]. Therefore, Raman spectroscopy is adopted to further investigate the structures of chars which are prepared by EP and EP/7.5% D-P-A after LOI tests. As shown in Fig. 8, there are two remarkable peaks at about 1360 and 1590 cm^{-1} in the both two spectra, which belong to D and G band, respectively. Generally, D band is owing to the vibrations of the amorphous char, and G band is ascribed to the vibration of sp^2-hybridized carbon atoms. Besides, the value of I_D/I_G (equals to A_D/A_G) is conversely proportional to the in-plane micro-crystalline size. As seen, the value of A_D/A_G for EP/7.5% D-P-A is 3.12, higher than 2.49 of EP, indicating a smaller size of carbonaceous microstructure. Based on this, the char layer of EP/7.5% D-P-A is considered to be a higher protective shield, which contributes to flame retard epoxy resin.

Moreover, the chemical compositions of char residues for EP and EP/7.5% D-P-A after LOI tests are further analyzed by X-ray photoelectron spectroscopy (XPS). The C_{1s}, N_{1s}, O_{1s}, P_{2p} and S_{2p} spectra of the samples are illustrated in Fig. 9. From the C_{1s} spectra, it suggests that there are three binding states of carbon in the char residues of EP and EP/7.5%D-P-A. Therein, the peak at 284.6 eV belongs to the C-H and C-C bonds in aliphatic and aromatic components, the peak at 285.8 eV is assigned to the C-O-C, C-OH, and C-N, and the peak at 289.7 eV is attributed to carboxyl group [37]. While the peak intensities at 285.8 eV for EP/7.5%D-P-A increase compared to EP, implying that more chars with cross-linking structure composed of C-O or C-N are formed. Fig. 9 (b) shows the N_{1s} spectra of EP and EP/7.5% D-P-A. Both present two peaks at 399.3 and 400.3 eV, wherein the former is assigned to C-N bond in pyridinic group, and the latter is the contribution in the pyrrolic group [38]. While it is noted that the peak intensity at 399.3 eV increases to some extent for EP/7.5 D-P-A, which might be ascribed to the formation of N-P bond. In the O_{1s} spectra of EP and EP/7.5% D-P-A, the peak at 532.0 eV is attributed to C = O and P = O in the carbonyl and phosphate group, and the peak at 533.0 eV is ascribed to –O- in C-O-C, C-O-P, P-O-P, and C-OH groups [39]. It is found that EP and EP/7.5% D-P-A differ in the peak intensity, which suggests that there is less oxidation of epoxy resin in the existence of D-P-A. Fig. 9 (d) and **(e)** show the P_{2p} and S_{2p} spectra of EP/7.5% D-P-A, and two peaks at 134.3 and 133.2 eV are assigned to P-O-C, P-O-P and/or PO_3^- group in phosphate. While, there is no signal of sulfur in the S_{2p} spectrum, indicating sulfur

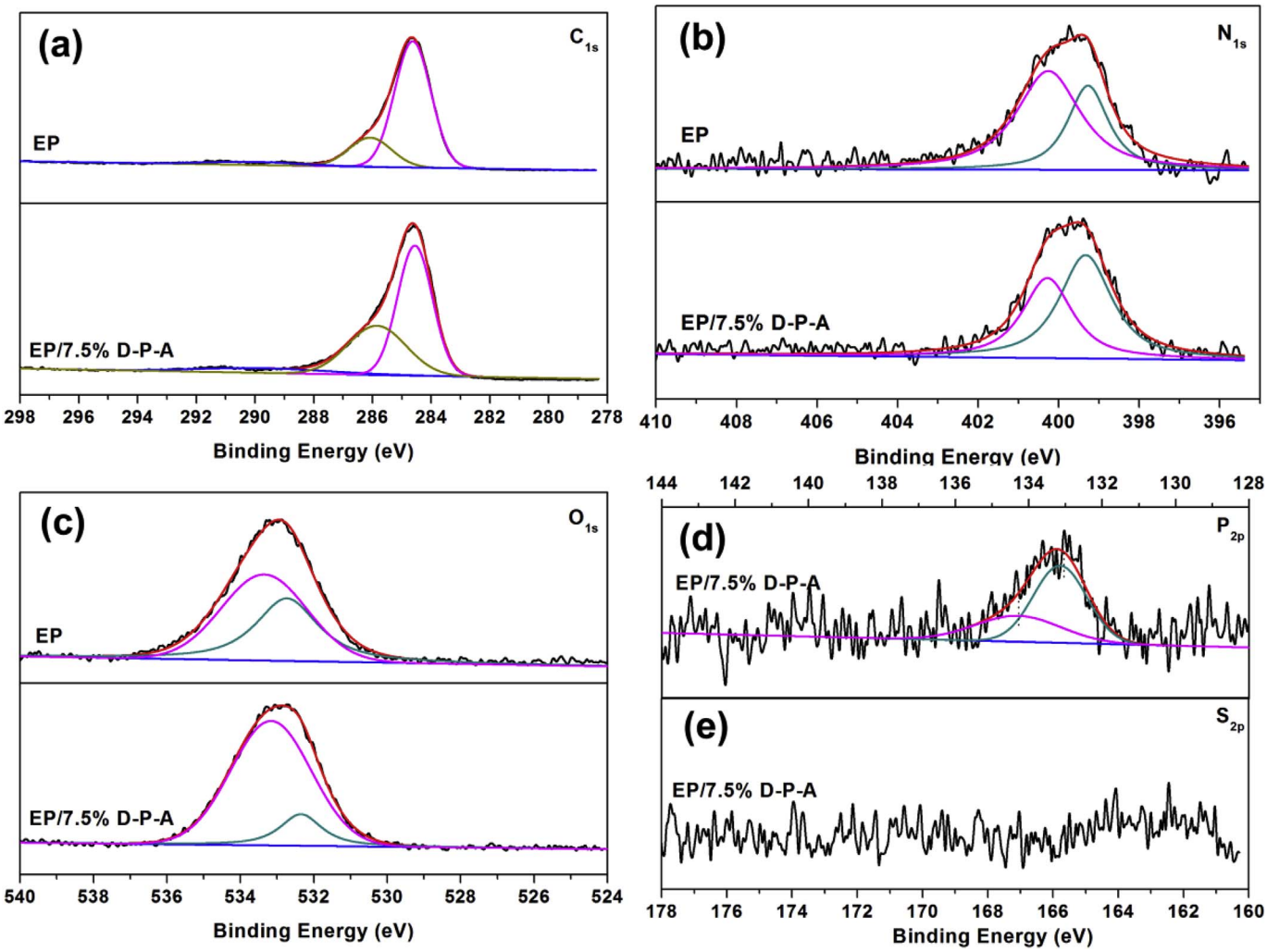

Fig. 9. XPS spectra of the chars of EP and EP/7.5% D-P-A after LOI testing.

element does not exist in the solid phase and no sulfur-containing products generate. It is deduced that sulfur works in the gaseous phase rather than condensed phase. Therefore Py-GC/MS is adopted to analyze the volatiles of D-P-A.

3.4.2. Gas-phase products analyses

As is well known, DOPO or DOPO-based derivatives work in the gaseous phase by generating phosphorus containing free radicals [1,16,23]. Therefore, the volatiles of D-P-A are analyzed by Py-GC/MS, and the total ion chromatogram (TIC) and GC/MS spectra are presented in Fig. 10. It is found that the main pyrolysis products of D-P-A are benzene, toluene, phenol, p-hydroxy toluene, benzothiazole, biphenyl, *o*-phenylphenol, fluorene, 2-aminobenzothiazole, and 9-phenyl fluorene. It is believable that the fragments such as benzene, toluene, phenol, p-hydroxy toluene are derived from the part of PHBA. Besides, biphenyl, fluorene, *o*-hydroxybiphenyl and 9-phenyl fluorene are originated from DOPO moiety, and it suggests the pyrolysis of phosphaphenanthrene also leads to the release of the phosphorus-containing fragments. Furthermore, these phosphorus-containing fragments can produce free radicals including PO· and PO_2· to capture the H· and HO· generating in the flame. Moreover, since sulfur element is not detected in the solid phase, it is speculated that benzothiazole and 2-aminobenzothiazole would further generate nitrogen/sulfur-containing compounds such as ammonia, sulfur dioxide and so on which can exert oxygen-diluting effect during combustion.

Based on the analyses above, it is concluded that D-P-A not only improves the quality of char residues which are more continuous and compact, but also exerts inert gas such as ammonia, sulfur-containing gas and phosphorus-containing free radicals to dilute oxygen. Consequently, epoxy resin is flame-retarded.

4. Conclusions

Flame retardant epoxy resin was successfully prepared through introducing a P/N/S-containing flame retardant. Owing to the lower thermal stability of D-P-A, it also caused the decreased thermal stability of epoxy resins. While EP/D-P-As passed a vertical UL-94 V-0 rating, and got higher LOI values in the loading of 7.5 wt% and 10 wt%. Moreover, the heat release of epoxy resin was suppressed, thanks to binary flame retardant activity of D-P-A in both gas and condensed phase. On the one hand, D-P-A generated inert gases such as ammonia and sulfur dioxide to dilute the oxygen, and phosphorus-containing free radicals to interrupt free radical reaction. On the other hand, during combustion, EP/D-P-As formed more continuous and compact char residues, which acted as a barrier to inhibit the transfer of heat and oxygen.

Acknowledgements

Financial supports from the National Natural Science Foundation of China (Grant No. 21504015, 51403040) and the Natural Science Foundation of Fujian Province of China (No. 2015J05094), would be

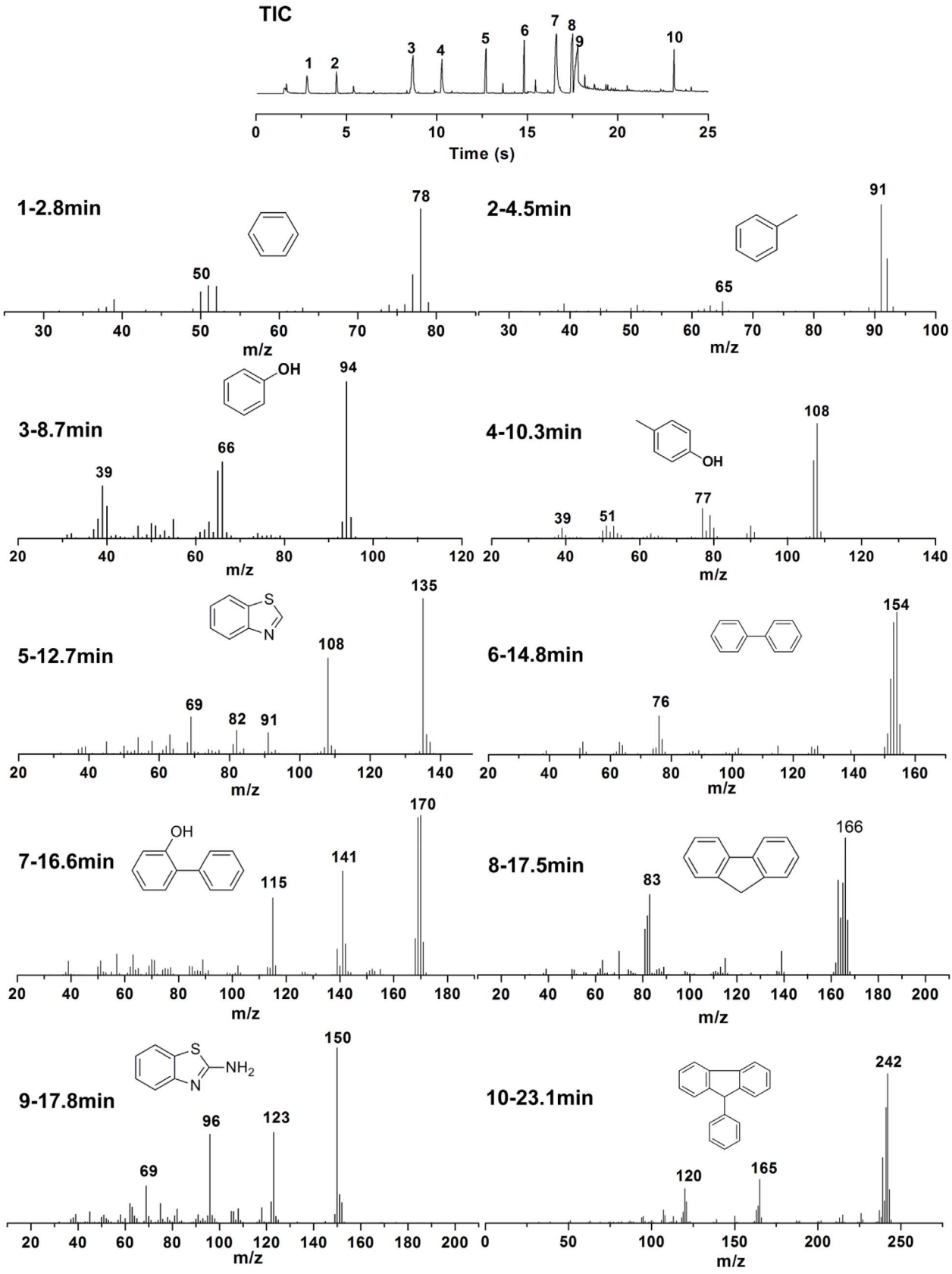

Fig. 10. TIC and GC/MS spectra of main pyrolysis products of D-P-A.

sincerely acknowledged.

References

[1] E.D. Weil, S. Levchik, A review of current flame retardant systems for epoxy resins, J. Fire Sci. 22 (2004) 25–40.
[2] F.L. Jin, X. Li, S.J. Park, Synthesis and application of epoxy resins: a review, J. Ind. Eng. Chem. 29 (2015) 1–11.
[3] S. Wang, S. Ma, C. Xu, Y. Liu, J. Dai, Z. Wang, X. Liu, J. Chen, X. Shen, J. Wei, Vanillin-derived high-performance flame retardant epoxy resins: facile synthesis and properties, Macromolecules 50 (2017) 1892–1901.
[4] O. Mauerer, New reactive, halogen-free flame retardant system for epoxy resins, Polym. Degrad. Stabil. 88 (2005) 70–73.
[5] H.B. Zhao, Y.Z. Wang, Design and synthesis of PET-based copolyesters with flame-retardant and antidripping performance, Macromol. Rapid Commun. (2017) 1700451.
[6] H.B. Zhao, Z.B. Fu, H.B. Chen, M. Zhong, C.Y. Wang, Excellent electromagnetic absorption capability of ni/carbon based conductive and magnetic foams synthesized via green one pot route, ACS Appl. Mater. Interfaces 8 (2016) 1468–1477.
[7] R. Yang, L. Chen, W.Q. Zhang, H.B. Chen, Y.Z. Wang, In situ reinforced and flame-retarded polycarbonate by a novel phosphorus-containing thermotropic liquid crystalline copolyester, Polymer 52 (2011) 4150–4157.
[8] Z. Li, L. Liu, A.J. González, D.Y. Wang, Bioinspired polydopamine-induced assembly of ultrafine Fe(OH)3 nanoparticles on halloysite toward highly efficient fire retardancy of epoxy resin via an action of interfacial catalysis, Polym. Chem. 8 (2017) 3926–3936.
[9] E.N. Kalali, X. Wang, D.Y. Wang, Multifunctional intercalation in layered double hydroxide: toward multifunctional nanohybrids for epoxy resin, J. Mater. Chem. 4 (2016) 2147–2157.
[10] X. Wang, E.N. Kalali, J.T. Wan, D.Y. Wang, Carbon-family materials for flame retardant polymeric materials, Prog. Polym. Sci. 69 (2017) 22–46.
[11] C. Ma, B. Yu, N. Hong, Y. Pan, W. Hu, Y. Hu, Facile synthesis of a highly efficient, halogen-free and intumescent flame retardant for epoxy resins: thermal properties, combustion behaviors and flame retardant mechanisms, Ind. Eng. Chem. Res. 55 (2016) 10868–10879.
[12] L.P. Gao, D.Y. Wang, Y.Z. Wang, J.S. Wang, B. Yang, A flame-retardant epoxy resin based on a reactive phosphorus-containing monomer of dodpp and its thermal and flame-retardant properties, Polym. Degrad. Stabil. 93 (2008) 1308–1315.
[13] B. Zhao, W.J. Liang, J.S. Wang, F. Li, Y.Q. Liu, Synthesis of a novel bridged-cyclotriphosphazene flame retardant and its application in epoxy resin, Polym. Degrad. Stabil. 133 (2016) 162–173.
[14] X. Zhao, H.V. Babu, J. Llorca, D.Y. Wang, Impact of halogen-free flame retardant with varied phosphorus chemical surrounding on the properties of diglycidyl ether of bisphenol-A type epoxy resin: synthesis, fire behaviour, flame-retardant mechanism and mechanical properties, RSC Adv. 6 (2016) 59226–59236.
[15] L. Qian, L. Ye, Y. Qiu, S. Qu, Thermal degradation behavior of the compound containing phosphaphenanthrene and phosphazene groups and its flame retardant mechanism on epoxy resin, Polymer 52 (2011) 5486–5493.
[16] L.J. Qian, L.J. Ye, G.Z. Xu, J. Liu, J.Q. Guo, The non-halogen flame retardant epoxy resin based on a novel compound with phosphaphenanthrene and cyclotriphosphazene double functional groups, Polym. Degrad. Stabil. 96 (2011) 1118–1124.
[17] Y. Qiu, V. Wachtendorf, P. Klack, L. Qian, Z. Liu, B. Schartel, Improved flame retardancy by synergy between cyclotetrasiloxane and phosphaphenanthrene/triazine compounds in epoxy thermoset, Polym. Int. (2017) 1883–1890.
[18] W. Zhang, X. Li, R. Yang, Study on flame retardancy of TGDDM epoxy resins loaded with DOPO-POSS compound and ops/dopo mixture, Polym. Degrad. Stabil. 99 (2014) 118–126.
[19] W. Zhang, X. Li, H. Fan, R. Yang, Study on mechanism of phosphorus–silicon synergistic flame retardancy on epoxy resins, Polym. Degrad. Stabil. 97 (2012) 2241–2248.
[20] S. Song, J. Ma, K. Cao, G. Chang, Y. Huang, J. Yang, Synthesis of a novel dicyclic silicon-/phosphorus hybrid and its performance on flame retardancy of epoxy resin, Polym. Degrad. Stabil. 99 (2014) 43–52.
[21] M. Xu, W. Zhao, B. Li, K. Yang, L. Lin, Synthesis of a phosphorus and sulfur-containing aromatic diamine curing agent and its application in flame retarded epoxy resins, Fire Mater. 39 (2015) 518–532.
[22] J. Wagner, P. Deglmann, S. Fuchs, M. Ciesielski, C.A. Fleckenstein, M. Döring, A flame retardant synergism of organic disulfides and phosphorous compounds, Polym. Degrad. Stabil. 129 (2016) 63–76.
[23] R. Jian, P. Wang, L. Xia, X. Yu, X. Zheng, Z. Shao, Low-flammability epoxy resins with improved mechanical properties using a lewis base based on phosphaphenanthrene and 2-aminothiazole, J. Mater. Sci. 52 (2017) 1–15.
[24] K. Zhou, R. Gao, X. Qian, Self-assembly of exfoliated molybdenum disulfide (MoS_2) nanosheets and layered double hydroxide (LDH): towards reducing fire hazards of epoxy, J. Hazard Mater. 338 (2017) 343–355.
[25] Y. Zhang, B. Yu, B. Wang, K.M. Liew, L. Song, C. Wang, Y. Hu, Highly effective P-P synergy of a novel DOPO-based flame retardant for epoxy resin, Ind. Eng. Chem. Res. 56 (2017) 1245–1255.
[26] W. Yan, J. Yu, M. Zhang, S. Qin, T. Wang, W. Huang, L. Long, Flame-retardant effect of a phenethyl-bridged DOPO derivative and layered double hydroxides for epoxy resin, RSC Adv. 7 (2017) 46236–46245.
[27] C. Klinkowski, S. Wagner, M. Ciesielski, M. Döring, Bridged phosphorylated diamines: synthesis, thermal stability and flame retarding properties in epoxy resins, Polym. Degrad. Stabil. 106 (2014) 122–128.
[28] B. Schartel, A.I. Balabanovich, U. Braun, U. Knoll, J. Artner, M. Ciesielski, M. Döring, R. Perez, J.K.W. Sandler, V. Altstädt, Pyrolysis of epoxy resins and fire behavior of epoxy resin composites flame-retarded with 9,10-dihydro-9-oxa-10-phosphaphenanthrene-10-oxide additives, J. Appl. Polym. Sci. 104 (2010) 2260–2269.
[29] A. Wirasaputra, X. Yao, Y. Zhu, S. Liu, Y. Yuan, J. Zhao, Y. Fu, Flame-retarded epoxy resins with a curing agent of DOPO-triazine based anhydride, Macromol. Mater. Eng. 301 (2016) 982–991.
[30] M. Rakotomalala, S. Wagner, M. Döring, Recent developments in halogen free flame retardants for epoxy resins for electrical and electronic applications, Materials 3 (2010) 4300–4327.
[31] P. Wang, Z. Cai, Highly efficient flame-retardant epoxy resin with a novel DOPO-based triazole compound: thermal stability, flame retardancy and mechanism, Polym. Degrad. Stabil. 137 (2017) 138–150.
[32] R.K. Jian, P. Wang, W. Duan, J.S. Wang, X. Zheng, J. Weng, Synthesis of a novel P/N/S-containing flame retardant and its application in epoxy resin: thermal property, flame retardance and pyrolysis behavior, Ind. Eng. Chem. Res. 55 (2016) 11520–11527.
[33] R. Jian, P. Wang, L. Xia, X. Zheng, Effect of a novel P/N/S-containing reactive flame retardant on curing behavior, thermal and flame-retardant properties of epoxy resin, J. Anal. Appl. Pyrol. 127 (2017) 360–368.
[34] B. Schartel, T.R. Hull, Development of fire-retarded materials—interpretation of cone calorimeter data, Fire Mater. 31 (2010) 327–354.
[35] A. Sadezky, H. Muckenhuber, H. Grothe, R. Niessner, U. Pöschl, Raman microspectroscopy of soot and related carbonaceous materials: spectral analysis and structural information, Carbon 43 (2005) 1731–1742.
[36] R. Yang, B. Ma, H. Zhao, J. Li, Preparation, thermal degradation and fire behaviors of intumescent flame retardant polypropylene with a charring agent containing pentaerythritol and triazine, Ind. Eng. Chem. Res. 55 (2016) 5298–5305.
[37] J.S. Wang, D.Y. Wang, Y. Liu, X.G. Ge, Y.Z. Wang, Polyamide-enhanced flame retardancy of ammonium polyphosphate on epoxy resin, J. Appl. Polym. Sci. 108 (2010) 2644–2653.
[38] S. Bourbigot, M.L. Bras, R. Delobel, L. Gengembre, XPS study of an intumescent coating. II. Application to the ammonium polyphosphate/pentaerythritol/ethylenic terpolymer fire retardant system with and without synergistic agent, Appl. Surf. Sci. 120 (1997) 15–29.
[39] W.J. Liang, B. Zhao, P.H. Zhao, C.Y. Zhang, Y.Q. Liu, Bisphenol-S bridged penta (anilino)cyclotriphosphazene and its application in epoxy resins: synthesis, thermal degradation, and flame retardancy, Polym. Degrad. Stabil. 135 (2017) 140–151.